

# Determining Fracture Characteristics in Scalpel Cutting of Soft Tissue<sup>\*</sup>

Teeranoot Chanthasopeephan, Jaydev P. Desai<sup>†</sup>, and Alan C.W. Lau  
*Program for Robotics, Intelligent Sensing, and Mechatronics (PRISM) Laboratory*  
*Drexel University*  
*Philadelphia, PA 19104*  
*Email: {teeranoo, desai, alau}@coe.drexel.edu*

**Abstract** This paper addresses the characteristic response of soft tissue to the growth of a cut (cracking) with a scalpel blade. We present our experimental equipment, experiments, and the results for scalpel cutting of soft tissue. The experimentally measured cut-force versus cut-length data was used to determine the soft tissue's resistance to fracture (resistance to crack extension) in scalpel cutting. The resistance to fracture (the toughness) of the soft tissue is quantified by the measure  $R$  defined as the amount of mechanical work needed to cause a cut (crack) to extend for a unit length in a soft-tissue sample of unit thickness. The equipment, method, and model are applicable for all soft tissue. We used pig liver as soft-tissue samples for our experiments.

**Index Terms** – Fracture Resistance, Toughness, Soft Tissue, Fracture Characteristics, Surgical simulation, Haptic Display

## I. INTRODUCTION

The mechanical property of soft biological tissue is of interest to many researchers. The deformation of soft tissue can frequently be characterized as nonlinear, viscoelastic and incompressible [1]. In a recent study, the deformation of the soft tissue of pig liver was shown to exhibit a nonlinear J-shape relationship between stress and strain [2]. To enable realistic haptics display for development of surgery simulator and robotic surgery, it is essential to quantify not only the deformation characteristics of soft tissue but also its response to various modalities of surgical cutting. In this regard, one important property of interest is the resistance to fracture (the toughness or resistance to cracking) of the soft tissue.

Griffith described fracture mechanics as a balance between the external work and the internal strain energy [3]. Doran et al [4] experimentally measured the resistance to fracture of biological membrane. They used a simplified model of stress/strain behavior of the tissue where it was assumed that no strain energy was stored in the skin until a certain level of strain was reached. The membrane deformed in front of the blade until cutting occurred. Oyen-Tiesma and Cook [5] determined fracture resistance of cultured neocartilage using energy based method. The experiment was done on cyclic tension tests for notched and un-notched samples. The dissipated energy was calculated through the integration of the area under the load-displacement curve during loading and unloading of each cycle. The amount of energy dissipated due to fracture was determined by the total measured dissipated energy minus the energy dissipated due to viscoelasticity (predicted). Fracture resistance then was calculated from fracture energy per cycle over the thickness times crack-length while viscoelastic work was estimated through the actual load curve and an estimated unload curve. Purslow [6] studied the non-linear elasticity on the toughness of soft tissue measured by tear tests. The test was done on specimens of J-shape stress/strain material such as the mesogloea, rat skin, pig aorta and R-shape stress/strain material such as cooked meat. The nature of load-deformation curve of a tear test appeared to influence the behavior of the fracture. The strain energy stored in the legs of specimen during tear test was also studied and found to be a critical factor during crack growth.

Kendall and Fuller [7] found that non-linearity had little influence on certain cracking test such as trouser tear test but the contribution part was instead from fracture surface energy. Mai and Atkins [8] performed a similar test on tear test to study the nonlinear fracture toughness of material. However, Mai and Atkins believed that the deformation of the legs before fracture played significant role in the

---

<sup>\*</sup> This work is supported by NSF Grant 0133471 and 0312709.

<sup>†</sup> Corresponding author

nonlinear stress-strain properties of fracture toughness. On the other hand, the assumption in [7] was that the strain energy stored in the legs of a deformed tear test specimen was insignificant.

With regard to fracture characteristics in cutting of soft tissue, Mai and Atkins [8] performed guillotine cutting in order to study mechanics during cutting with blade. Darvell and co-workers [9] proposed a portable fracture toughness machine for scissors or wedge tests. Mahvash and Hayward [10] presented a fracture-mechanics approach to calculate the force during cutting of soft tissue for haptic rendering of cutting. Pereira et al [11] studied fracture mechanics of soft tissue during scissor cutting test. Scissor cutting is different from blade cutting by adding the shear mode into fracture. The energy method was also used to determine the fracture resistance during scissor cutting. The viscoelastic effect was negligible in this case. Ahsan et al [12] used energy based method to study the fracture of biological material. They performed peel test, shear test (Mode II), tear test (Mode III) along with estimated fracture toughness from energy release rates. Chin-Purcell et al [13] applied the Modified Single Edged Notch (MSEN) test method and tear test method for the fracture of articular cartilage. They compared the MSEN method to the trouser tear test. The trouser tear test method allowed fracture analysis for mode III crack growth.

A stress intensity approach for fracture mechanics was also done by Adeeb et al [14]. They studied the fatigue behavior of tendon tissue based on tension testing and cyclic loading experiment. The nonlinearity was negligible along with the fracture process zone at flaw tip. The stress intensity was assumed constant throughout the tendon. The fracture toughness of the tendon was related to its ultimate tensile stress.

Fracture toughness was also determined using a micropenetration technique introduced by Simha et al [15]. The toughness of the material (in this experiment cartilage) was the resistance of the tissue to penetration. They defined toughness as the ratio of the penetration work to one-half of the surface area of a cone with depth  $pen$ , the penetration depth. Most of the analyses used quasi-static analysis.

## II METHOD

### *Experimental set up for determining the liver Fracture Resistance (toughness) during cutting*

The equipment consists of a scalpel-blade cutting subsystem, a computer control subsystem, a digital data-acquisition subsystem, and a data post-processing subsystem (see figure 1). The test equipment to measure the liver cutting forces was designed to variable cutting speed to measure the effect of cutting speed on cutting forces and strain rates within the specimen (speeds can be varied from 0 to 3.81cm/second).

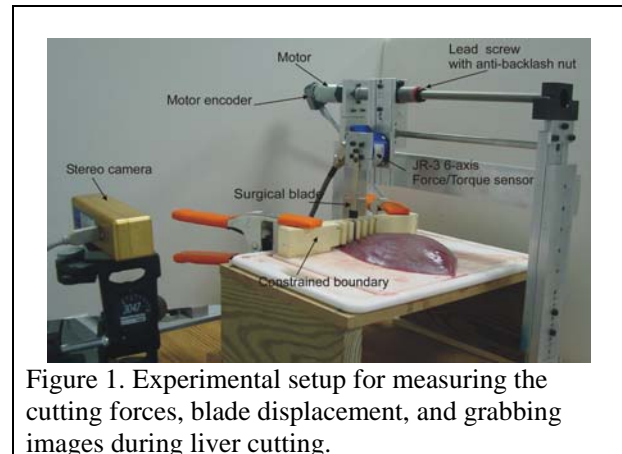


Figure 1. Experimental setup for measuring the cutting forces, blade displacement, and grabbing images during liver cutting.

The constrained boundary shown in the figure was designed to simulate the attachment of the liver on one end as in a human body (such as the attachment to the diaphragm). The entire cutting mechanism consists of two vertical supports, a lead screw assembly with a geared DC motor and an incremental encoder (manufactured by Maxon Motors, model A-max32 with planetary gearhead GP 32C and digital encoder HEDL 55 with line driver RS 422), and a JR3 precision 6-axis force/torque sensor (model 85M35A-I40, with worst case resolution of 0.05 N in  $F_x$  and  $F_y$ , 0.1 N in  $F_z$  and 0.00315 Nm in  $T_x$ ,  $T_y$  and  $T_z$ ) to which a surgeon's scalpel is attached. We used #10 Bard-Parker stainless steel surgical blade in our experimental studies, consistent with what is used by surgeons. The cutting blade traverses linearly based on the rotary motion of the DC motor. An anti-backlash nut connects the lead screw to the force sensor. The scalpel was screwed to the force sensor and the force sensor was mounted on an aluminum plate with one end attached to the anti-backlash nut traveling along the lead screw and the other end on a lower guiding shaft (parallel to the lead screw) with a linear bearing to provide low friction linear travel. The design and construction of the cutting assembly ensured that the system was sufficiently rigid with no backlash so that the forces recorded by the force sensor are those obtained by cutting the tissue alone. A bumble bee stereo camera system is arranged at 30cm in front of

the experimental setup to enable subsequent image-processing of the depth of the surgical blade embedded in the liver sample at each instant of the cutting process. The dSPACE DS1103 controller board (manufactured by dSPACE, Inc.) recorded the position and force data from the motor's encoder and force sensor in real-time along with grabbing images at the rate of 13 frames/second. We have implemented a proportional + derivative (PD) controller to enable precise movement of the motor (and hence the cutting blade during cutting tasks).

### 2.1 Experimental procedure for measuring liver cutting forces

Since the experiments were performed on ex-vivo liver tissue, the preparation of the tissue before the experiment helped maintain the properties of the tissue as close as possible to the in-vivo properties. We transported the liver from freshly slaughtered pigs to our laboratory within 2 hours post mortem. The liver tissue sample was not preconditioned because in surgery, the cutting forces experienced by the surgeon are on non-preconditioned tissues. Before starting the experiment, we cut the pig's liver into specimens of size 8x15x2.5cm. The outer encapsulated surface was not cut since we were interested in measuring the cutting forces on the liver. The outer rim of the specimen was covered with petroleum jelly to minimize moisture loss during the experiment. A bar of rectangular shape made of machineable plastic with an array of small nails clamped at the bottom end penetrated through one edge of the liver specimen to simulate a single constrained boundary surface. While this is not an exact replication of the boundary conditions for a human liver (which is partially attached on one end to the diaphragm) this is none-the-less a valid simplification for our initial tests and model (based on our discussions with surgeon collaborators). The cutting velocity was set at 0.1cm/sec (quasi-static cutting speed). The force exerted on the blade by the tissue was continuously recorded by The JR3 precision 6-axis force/torque sensor attached to the scalpel. By Newton's law of action and reaction, the cutting blade exerted the same magnitude of force on the soft tissue being cut.

### 2.2 Determination of depth of cut

The depth of cut plays significant role in the magnitude of the cut force sensed at the blade. We used images to analyze how deep the blade was embedded inside the liver specimen at each instant of

the cutting process. We used Point Grey's Bumblebee stereo camera system to grab snap shots of cutting (Figure 2) at 13 frames/second. The images were then post-processed with Matlab 6.5 image processing toolbox to track the center of the black rectangular box (Figure 2), which was on the top of the cutting blade. Then using edge detection, we were able to detect the liver surface. The distance from the center of the rectangular box and the surface of the liver is measured in term of pixel. Since the position of the center of the box to the tip end of the blade is 4 cm, we thus can determine the depth of the

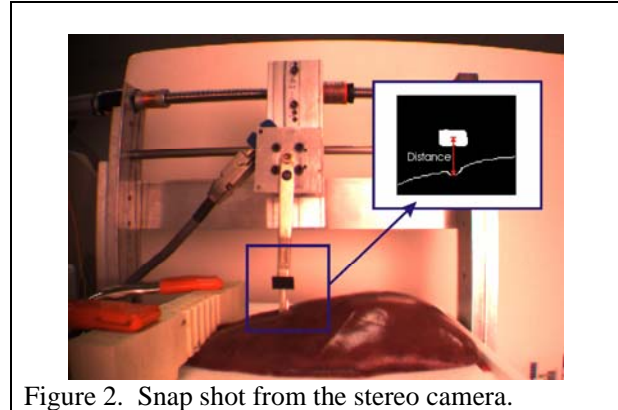


Figure 2. Snap shot from the stereo camera.

blade embedded in the liver (the depth of cut) through conversion from pixel to length expressed in centimeter.

### 2.3 Determination of fracture resistance

Figure 3 shows schematically a liver specimen

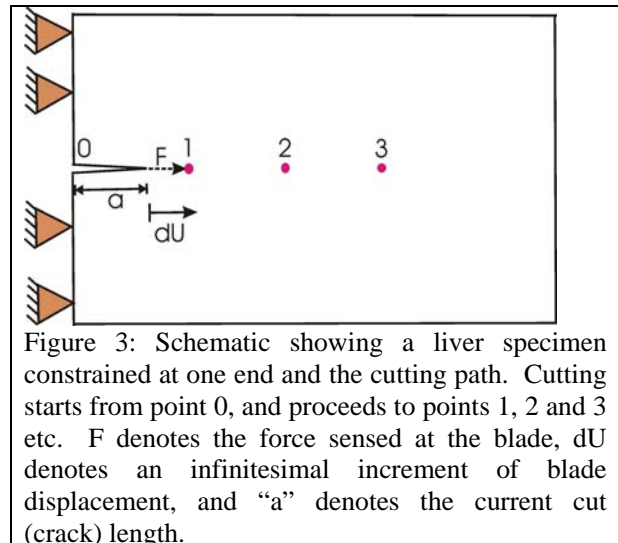


Figure 3: Schematic showing a liver specimen constrained at one end and the cutting path. Cutting starts from point 0, and proceeds to points 1, 2 and 3 etc. F denotes the force sensed at the blade, dU denotes an infinitesimal increment of blade displacement, and "a" denotes the current cut (crack) length.

constrained at one end and the cutting path. Cutting starts from point 0, and proceeds to points 1, 2 and 3 etc. F denotes the force sensed at the blade, dU denotes an infinitesimal increment of blade

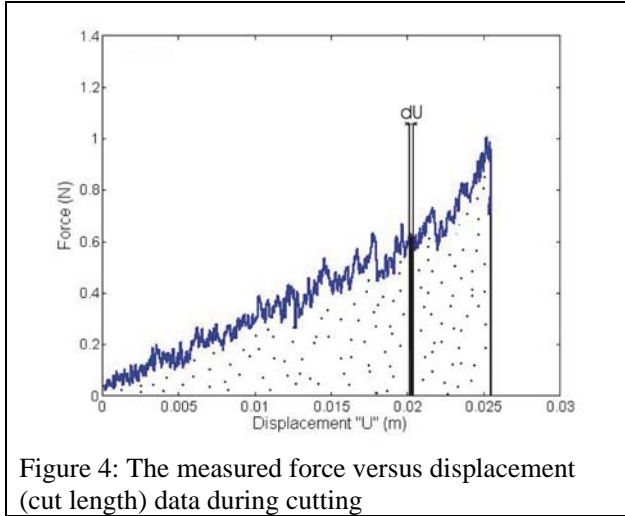


Figure 4: The measured force versus displacement (cut length) data during cutting displacement, and “a” denotes the current cut (crack) length.

Figure 4 shows the measured force versus the cut length (displacement of the blade). If at the instant when the force is  $F$  the blade moves an additional infinitesimal displacement of  $dU$ , the increment of externally exerted work done  $dW_{ext}$  is given by:

$$dW_{ext} = FdU \quad (1)$$

The externally applied work to move the cutting blade from the starting point to a final point over a total displacement of length ‘a’ is:

$$W_{ext} = \int_0^a dW_{ext} = \int_0^a FdU \quad (2)$$

Graphically,  $W_{ext}$  is depicted by the area beneath the force versus displacement curve in Figure 4. If we assume that all this externally applied work  $W_{ext}$  is used to pay for the fracture work (energy) barrier  $W_{fracture}$  that is required to enable the crack (the cut) grow from zero length to the length of ‘a’, then:

$$W_{fracture} = W_{ext} = \int_0^a FdU \quad (3)$$

The force  $F$  shown in Figure 4 is from raw experimental data where the blade was embedded at different depths in the soft tissue during the cutting. We can normalize the magnitude  $F$  with the instantaneous depth of cut to obtain the normalized cutting force for a soft tissue sample of unit thickness. From the resulting plot, we can obtain the work of fracture for cutting a crack of length ‘a’ in a soft tissue sample of *unit* thickness,  $W^*$ . The resistance to fracture of the soft tissue,  $R$ , can be defined as the amount of required fracture work to

cause a cut (crack) to extend for a unit length in a soft-tissue sample of unit thickness.

$$R = \frac{W_{fracture}^*}{a} \quad \dots\dots\dots(4)$$

The resistance to fracture,  $R$ , is a measure of the materials resistance to the extension (propagation) of a crack. The fracture resistance of a material is frequently also labeled as the fracture *toughness* of the material.

### III RESULTS

We performed 40 cutting experiments for various cutting lengths ranging from 0.5-4 inch. These experiments were designed to determine the magnitude of the fracture resistance (fracture

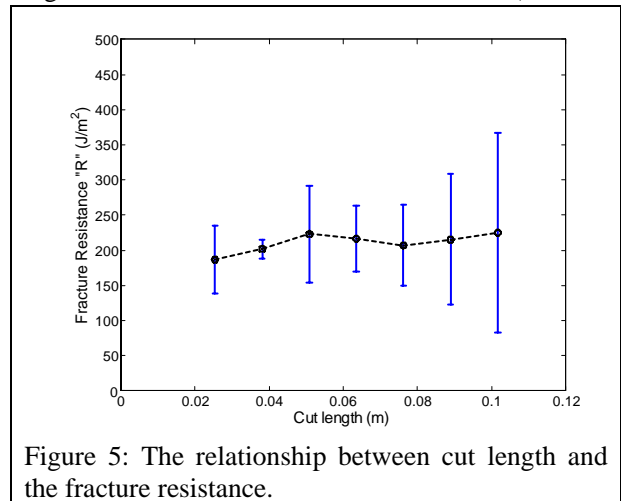


Figure 5: The relationship between cut length and the fracture resistance.

Cut length		Average fracture resistance “R” (J/m <sup>2</sup> )	Standard deviation
Inch	m		
1	0.0254	186.98	48.26
1.5	0.0381	201.72	13.67
2	0.0508	223.06	68.93
2.5	0.0635	216.64	47.24
3	0.0762	207.08	57.60
3.5	0.0889	215.39	93.35
4	0.1016	224.83	142.01

Table 1: The average fracture toughness and the standard deviation from 40 cutting experiments

toughness), and to study whether the fracture resistance in this soft tissue varies with the crack length (the length of cut) as is the case in some ductile engineered materials. Figure 5 and Table 1 depict results of the fracture resistance of 40 liver cuttings determined at various cut length ranging between 0.127-0.1016 m (0.5-4 inch). The results

show that the magnitude of the average fracture resistance of the liver is ranging between  $187 \text{ J/m}^2$  and  $225 \text{ J/m}^2$ . It is also apparent that the fracture resistance of this soft tissue is not sensitive to crack length.

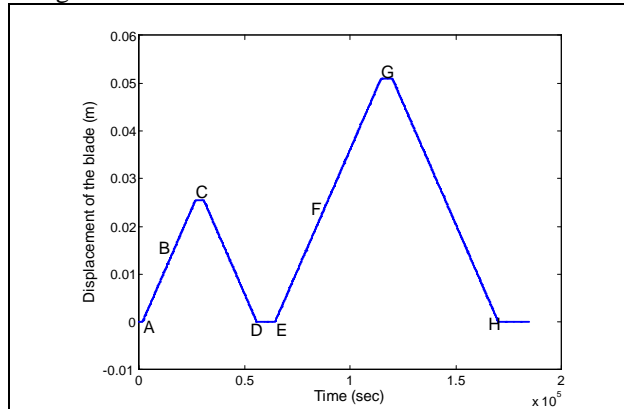


Figure 6: The travel profile of the displacement of the blade.

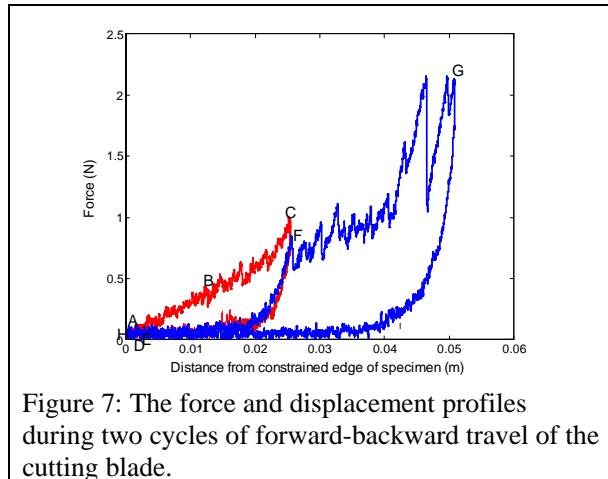


Figure 7: The force and displacement profiles during two cycles of forward-backward travel of the cutting blade.

Next we performed 10 experiments in each of which the blade traveled forward and backward for two cycles. In each experiment, we first let the blade move forward to cut the liver for 1 inch. After the blade moved forward and reached the specified cut length of one inch, the blade reversed its direction of travel and backward moved along the previous path to the starting point. In the backward (return) trip, the blade was not cutting but was traveling in the previously created one-inch “crack”.

After reaching the starting point, the blade then moved forward a second time: this time to travel forward for 2 inches. During this second forward travel, the blade first traveled for 1 inch in the previously-created “crack”, and then the blade cut for 1 inch in previously uncut liver tissue. At the end of the 2 inch travel, the blade stopped. The blade then reversed its direction of travel and returned to the

starting point by traveling along the two-inch “crack” just created.

Figure 6 shows the travel profile of the blade displacement. The corresponding force versus displacement profiles are portrayed in Figures 7 and 8. The red lines depict the first 1-inch loading-unloading (forward-backward movement) cycle. The blue curve corresponded to the second cycle with a travel distance of 2 inches. Figures 7 and 8 reveal two interesting features. During the return travel in

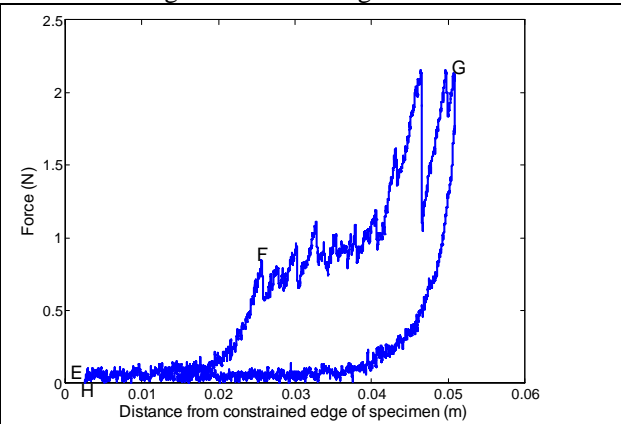


Figure 8: The force and displacement profile during the second cycle of the two forward-backward travel cycles of the cutting blade.

the first cycle, the blade was traveling in a previously created crack, but there was still force sensed by the blade. Apparently, the crack surfaces were in contact with the blade surface and exerted frictional force on the blade. In the second cycle, during the first inch of travel when the blade traveled forward in the crack, the blade experienced the same magnitude and variation of frictional force as it had experienced during the backward travel in the crack in the first cycle. After the first inch of travel in the crack, the force versus displacement curve reached approximately the unloading point of the first cycle. The subsequent cutting during the next inch of blade travel resulted in a loading force-displacement curve continuing approximately where the loading part of the first cycle left off.

#### IV CONCLUDING REMARKS

We presented the experiments and methods to determine the fracture characteristics the liver soft tissue in scalpel cutting. Using an energy balance approach to fracture mechanics, the resistance to fracture (the toughness) of the soft tissue is quantified by the measure  $R$  defined as the amount of mechanical work needed to extend the cut for a unit

length in a soft-tissue sample of unit thickness. In this approach, the fracture resistance  $R$  incorporated the effects of all the physical mechanisms taking place in the cracking process. No simplifying assumptions such as those limiting the deformation to be small, linear and time-independent were used. The experiments and method **are applicable for all soft tissue**. The specific magnitude of the fracture resistance and its trend reported here were derived from experiments using pig liver for soft-tissue samples.

#### REFERENCES

- [1] Y. C. Fung, *Biomechanics: Mechanical properties of living tissues*, Second edition ed. New York: Springer-Verlag, 1993.
- [2] T. Hu and J. P. Desai, "Characterization of soft-tissue material properties: Large deformation analysis," Proceeding of the Second International Symposium on Medical Simulation - Emerging Science|Enabling Technologies, Boston, MA, 2004.
- [3] T. L. Anderson, *Fracture Mechanics: Fundamentals and Applications*, 2nd edition ed: CRC Press, 1994.
- [4] C. F. Doran, B. A. O. McCormack, and A. Macey, "A Simplified Model to Determine the Contribution of Strain Energy in the Failure Process of Thin Biological Membranes during Cutting," *Strain International Journal for Strain Measurement*, vol. 40, pp. 173, 2004.
- [5] M. Oyen-Tiesma and R. F. Cook, "Technique for estimating fracture resistance of cultured neocartilage," *Journal of Materials Science: Material in Medicine*, vol. 12, pp. 327-332, 2001.
- [6] P. P. Purslow, "Fracture of non-linear biological materials: some observations from practice relevant to recent theory," *Journal of Physics D: Applied Physics*, vol. 22, pp. 854-856, 1989.
- [7] K. Kendall and K. N. G. Fuller, "J-Shaped stress/strain curves and crack resistance of biological materials," *Journal of Physics D: Applied Physics*, vol. 20, pp. 1596-1600, 1987.
- [8] A. G. Atkins and Y. W. Mai, *Elastic and Plastic Fracture: metals, polymers, ceramics, composites, biological materials*: Ellis Horwood Limited, 1985.
- [9] B. W. Darvell, P. K. D. Lee, T. D. B. Yuen, and P. W. Lucas, "A portable fracture toughness tester for biological materials," *Measurement Science and Technology*, vol. 7, pp. 954-962, 1996.
- [10] M. Mahvash and V. Hayward, "Haptic Rendering of Cutting: A Fracture Mechanics Approach," *Haptics-e, The Electronic Journal of Haptics Research (www.haptics-e.org)*, vol. 2, 2001.
- [11] B. P. Pereira, P. W. Lucas, and T. Swee-Hin, "Ranking the Fracture Toughness of Thin Mammalian Soft Tissue Using the Scissors Cutting Test," *Journal of Biomechanics*, vol. 30, pp. 91-94, 1997.
- [12] T. Ahsan and R. L. Sah, "Biomechanics of integrative cartilage repair," *Journal of OsteoArthritis Research Society International*, vol. 7, pp. 29-40, 1999.
- [13] M. V. Chin-Purcell and J. L. Lewis, "Fracture of Articular Cartilage," *Journal of Biomechanical Engineering*, vol. 118, pp. 545-555, 1996.
- [14] S. M. Adeeb, M. L. Zec, G. M. Thornton, C. B. Fracnk, and N. G. Shrive, "A Novel Application of the Principles of Linear Elastic Fracture Mechanics (LEFM) to the Fatigue Behavior of Tendon Tissue," *Journal of Biomechanical Engineering*, vol. 126, pp. 641-650, 2004.
- [15] N. K. Simha, C. S. Carlson, and J. L. Lewis, "Evaluation of fracture toughness of cartilage by micropennetration," *Journal of Materials Science: Material in Medicine*, vol. 12, pp. 631-639, 2003.